Biosensors and Bioelectronics 31 (2012) 151–156

Contents lists available at SciVerse ScienceDirect

Biosensors and Bioelectronics

journal homepage: www.elsevier.com/locate/bios

Pd nanoparticle assemblies—As the substitute of HRP, in their biosensing applications for H_2O_2 and glucose

Min Han, Suli Liu, Jianchun Bao, Zhihui Dai*

Jiangsu Key Laboratory of Biofunctional Materials, College of Chemistry and Materials Science, Nanjing Normal University, Nanjing, 210097, PR China

ARTICLE INFO

Article history:
Received 26 July 2011
Received in revised form
22 September 2011
Accepted 6 October 2011
Available online 3 November 2011

Keywords:
Pd nanoparticle assemblies
Substitute of HRP
Biosensor
H_2O_2
Glucose

ABSTRACT

The spherical porous Pd nanoparticle assemblies (NPAs) have been successfully synthesized by starch-assisted chemical reduction of Pd(II) species at room temperature. Such Pd NPAs are not simply used to enlarge the surface area and to promote the electron transfer. They also catalyze the reduction of H_2O_2 which are regarded as horseradish peroxidase (HRP) substitutes in electron transfer process. By using them as electrocatalysts, as low as 6.8×10^{-7} M H_2O_2 can be detected with a linear range from 1.0×10^{-6} to 8.2×10^{-4} M. Moreover, through co-immobilization of such Pd NPAs and glucose oxidase (GOx), a sensitive and selective glucose biosensor is developed. The detection principle lies on measuring the increase of cathodic current by co-reduction of dissolved oxygen and the in situ generated H_2O_2 during the enzymatic reaction. Under optimal conditions, the detection limit is down to 6.1×10^{-6} M with a very wide linear range from 4.0×10^{-5} to 2.2×10^{-2} M. The proposed biosensor shows a fast response, good stability, high selectivity and reproducibility of serum glucose level. It provides a promising strategy to construct fast, sensitive, stable and anti-interferential amperometric biosensors for early diagnosis and prevention of diabetes.

1. Introduction

Diabetes is a worldwide public health problem. This disease is caused by metabolic disorder due to insulin deficiency and hyperglycemia, which is reflected by the blood glucose concentration higher or lower than the normal range (4.4–6.6 mM) (Wang, 2008). For early diagnosis and effective control of diabetes, exploring and developing fast, sensitive and reliable methods to detect glucose are very important. This pursuit has stimulated a considerable amount of fascinating research and led to the presence of innovative detection strategies (Clark et al., 1962; Updike and Hicks, 1967; Niculescu et al., 2000; D'Orazio, 2003; Shi et al., 2003; Malhotra and Chaubey, 2003; Yu et al., 2003; Crouch et al., 2005; Forrow and Bayliff, 2005; Cosnier et al., 2006; Wang, 2008). The construction of bienzymatic peroxidase/oxidase amperometric biosensors has been considered as one of the attractive approaches for the test and continuous monitoring of glucose in blood samples (Ferri et al., 1998; Cosnier et al., 2000; Delvaux et al., 2005). In such configurations, H_2O_2 is detected through its horseradish peroxidase (HRP) mediated reduction. Although HRP usually shows high catalytic efficiency and selectivity, its activity is easy to reduce or loss (Breslow, 1995; Chattopadhyay and Mazumdar, 2000; Shoji and Freund, 2001). In order to foster strength and circumvent weakness of this approach, it is urgently needed to search for HRP substitute to develop newly "bienzyme" based amperometric biosensors.

Inspired from the structure (Barman, 1985) and catalytic pathway (Berglund et al., 2002) of HRP, the designed substitute or artificial catalyst for HRP should possess highly active metallic site and a complex and flexible 3D environment (Zecchina et al., 2007). The former is designed to decrease the activation barrier and to selectively recognize and bind a desired substrate. While the latter can be considered as an "entrance guard", which allows suitable substrate to access the active center as well as the release of desired products. In this sense, the noble metal nanoparticle (NPs) may be the ideal candidate material for substitution of HRP. The reasons are as follows: (i) noble metal NPs have a good electrical performance and biocompatibility which results in potential application in bioelectronics. (ii) They possess unique catalytic properties, which can catalyze a wide range of organic reactions with lower activation barrier (Haruta, 2005; Astruc et al., 2005; Hashmi and Hutchings, 2006; Yan et al., 2006; Enache et al., 2006; Yin and Liebscher, 2007; Min and Friend, 2007; Corma et al., 2007; Fillon et al., 2007; Tian et al., 2007; Si and Flytzani-Stephanopoulos, 2008; Alayoglu et al., 2008; Lim et al., 2009). As one of the important noble metals, Pd is known to catalyze many chemical reactions. Up to now, many efforts have been stimulated toward the design and synthesis of Pd NPs owing to their size- and shape- dependent electrocatalytic performance (Pandey et al., 2004; Lim et al., 2005; Huang et al., 2008; Lee et al., 2008; Mazumder and Sun,

* Corresponding author. Tel.: +86 25 83598280.
E-mail address: daizhihuii@njnu.edu.cn (Z. Dai).

0956-5663/$ – see front matter © 2011 Elsevier B.V. All rights reserved.
doi:10.1016/j.bios.2011.10.008

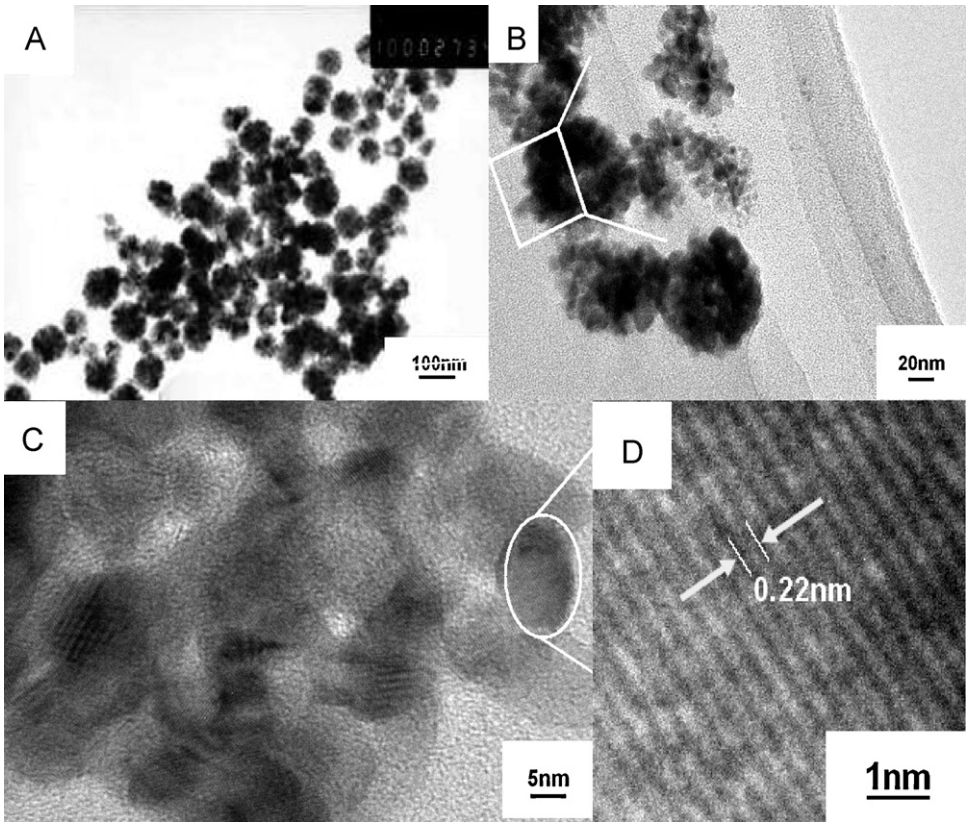

Fig. 1. Low (A) and high (B) magnification TEM images of the Pd NPAs. (C) High magnification TEM image of the edge section of an individual Pd NPAs marked by a white rectangular framework in (B). (D) HRTEM image of the building block of an individual Pd NPAs indicated by a white circle in (C).

2009; Huang et al., 2009; Ksar et al., 2009; Wang et al., 2009). Recently, our research group found that dendritic Pd nanostructures could electrocatalyze reduction of H_2O_2 which could be used to construct H_2O_2 biosensor (Zhou et al., 2007). Based on this work, we are interested in synthesis of various novel Pd nanostructures and investigation of their biosensing performance with the dream to find an ideal candidate material for the perfect substitute of HRP.

Herein, we report the synthesis of spherical porous Pd nanoparticle assemblies (NPAs) and their biosensing applications for H_2O_2 and glucose. The typical synthesis is based on hydrazine reduction of Pd(II) species at room temperature under the assistance of starch. The starch is a natural polymer of glucose and has a lot of polar head groups, which can stabilize and assemble the generated small Pd NPs to form large assemblies with spherical porous structure. The obtained spherical porous Pd NPAs have good adhesion ability on the electrode surface. Different from the previous reports (Dai et al., 2007; Li et al., 2010), no extra chitosan or Nafion is needed to fix Pd NPAs which is a remarkable advantage of our work. Such Pd NPAs not only increase the contact interface and promote the electron transfer but also catalyze the reduction of H_2O_2. Furthermore, through co-depositing of such Pd NPAs and glucose oxidase (GOx) on GCE, a sensitive and selective glucose biosensor can be constructed. Under optimal conditions, the detection limit is down to 6.1×10^{-6} M with a wide linear range from 4.0×10^{-5} to 2.2×10^{-2} M. In addition, the constructed biosensor shows a fast response, good stability, high selectivity and reproducibility of serum glucose level. The detections for H_2O_2 and glucose developed in this work show that the spherical porous Pd NPAs can be served as an ideal substitute of HRP, which may facilitate future design and fabrication of other easy-to-make and robust biosensors to apply in practical fields.

2. Experimental

2.1. Reagents

Reagents were described in electronic supplementary information (ESI).

2.2. Preparation of spherical porous Pd NPAs

0.51 g of $PdCl_2$ was dissolved in 12 mL of concentrated HCl, followed by adding 60 mL deionized water to make solution A. Then 0.5 mL solution A was added to 2 mL 6 g L^{-1} starch solution to make solution B. 0.2 mL hydrazine hydrate was added to 2 mL 6 g L^{-1} starch solution to make solution C. Then solution C was added to solution B under sonication for about 10 min and the black production was obtained. The deposit was washed with deionized water and ethanol several times. After vacuum drying, the black Pd NPAs were obtained. 3 mg of Pd NPAs was dispersed in 1 mL of deionized water to obtain the desired suspension with the concentration of 3 mg mL^{-1}.

2.3. Electrode preparation

GCE (3 mm in diameter) was polished to a mirror-like finish with 0.3 and 0.05 μm alumina slurry (Buhler, USA) followed by rinsing thoroughly with doubly distilled water. Then it was successively sonicated in acetone and doubly distilled water, and allowed to dry at room temperature. The GOx/Pd NPAs modified GCE was prepared by dropping 2 μL 3 mg mL^{-1} Pd NPAs suspension, and 2 μL of 3 mg mL^{-1} GOx on the surface of the electrode, respectively, and then allowed it to dry under ambient conditions for 3 h. When not in use the electrode was stored in 0.1 M pH 7.0 PBS at 4 °C. The Pd

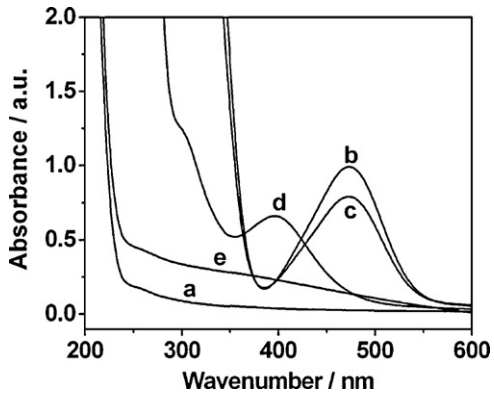

Fig. 2. UV–visible spectra of starch solution (a), H_2PdCl_4 solution (b), the mixture of H_2PdCl_4 and starch solution (c), the reaction systems before (d) and after (e) reaction for about 10 min.

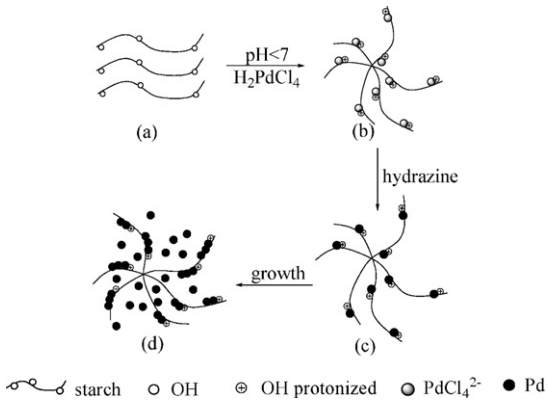

Scheme 1. An illustration of the possible formation procedure of Pd NPAs using starch as a template.

NPAs modified GCE was prepared by dropping 2 μL 3 mg mL^{-1} Pd NPAs suspension on GCE surface and then allowed it to dry under ambient conditions for 3 h in control experiment.

2.4. Apparatus and measurements

Apparatus and measurements were described in ESI.

3. Results and discussion

3.1. Structural characterization of Pd NPAs

The characterization of the obtained Pd NPAs is characterized by powder X-Ray diffraction (XRD). Corresponding XRD and energy dispersive X-Ray (EDX) spectra are shown in Fig. S1 in ESI.

The shape and microstructure of the obtained Pd NPAs are further examined by transmission electron microscopy (TEM), shown in Fig. 1. From the low magnification TEM image (Fig. 1A), large-areaed irregular spherical nanostructures with the average diameter of 40–60 nm can be observed. Corresponding high magnification TEM image (Fig. 1B) indicates that the observed large irregular spherical Pd nanostructures are composed of many small NPs, which are organized to form a sphere-like microstructure and left voids between the adjacent NPs. That is to say, the observed spherical Pd nanostructures are virtually porous NPAs. Further magnifying the edge section (as the white rectangular framework indicated in Fig. 1B) of an individual Pd NPAs, we can see many small ellipsoid-like nanostructure (Fig. 1C), implying that the building blocks of the Pd NPAs are nano-ellipsoids. The diameter of their short axis and long axis are about 3.4–8 nm and 6–15 nm, respectively. Moreover, some of the nano-ellipsoid units are fused together to produce nano cavity or pore-like structures, favoring for adsorption of catalytic substrates and desorption of desired product. The HRTEM analysis of the nano-ellipsoid building block (Fig. 1D) gives clear lattice fringes and the lattice spacing is about 2.20 Å, corresponding to the interplanar (1 1 1) distance of face-centered cubic phase Pd. Nitrogen adsorption–desorption isotherms demonstrate that Brunauer–Emmett–Teller (BET) surface area of the porous tubular nanostructure is about 65 $m^2\,g^{-1}$ and the major pore diameters are about 3 nm (Fig. S2 in ESI).

3.2. Growth mechanism of Pd NPAs

To learn about the growth mechanism of Pd NPAs, the UV–visible spectra of the solution before and after the reaction are recorded, respectively (Fig. 2). There is no absorption peak in starch solution (curve a) and an obvious absorption peak at about 474 nm in H_2PdCl_4 solution (curve b). When starch solution and H_2PdCl_4 solution is mixed, the relative intensity of the peak at 474 nm reduces due to the decrease of H_2PdCl_4 concentration and no new absorption peak appears (curve c), indicating that the interactions between starch molecule and H_2PdCl_4 is not strong and no new coordination bond is formed. When adding hydrazine to the mixture of starch and H_2PdCl_4, a new peak at about 397 nm can be observed (curve d), revealing the formation of complex between hydrazine and palladium (II) ions. The complex can be reduced by excessive hydrazine to generate Pd (0) nuclei. Prolonging the reaction time, the relative intensity of the peak at 397 nm gradually decreases (curve e), indicating that palladium (II) ions are gradually reduced to Pd (0) and used for the growth of crystal nuclei. After reaction for about 10 min, the peak at 397 nm completely disappears, confirming that the palladium salt is fully reduced. Thus, we can infer that the obtained spherical porous Pd NPAs may be formed by continuous reduction of unreacted Pd (II) ions and subsequent deposition of Pd (0) cluster on initially formed Pd seeds to generate small ellipsoid-like NPs. In order to decrease the surface energy, those small NPs will be in situ organized into large spherical assemblies under the assistance of starch. The starch can be acted as a template (structure directing agent) for the growth of nanoparticles (Yang et al., 2005; Zhang et al., 2011). In our experiment, at the beginning stage of the reaction, the system is acidic. So, the hydroxyl groups of starch might be protonized, which can enrich the $PdCl_4^{2-}$ anions and subsequently favor the nucleation and growth of Pd along the molecular chain of the starch. From Fig. 1C, we can see that the adjacent nanoparticles were fused due to their same crystal orientation (Zhou et al., 2007) which caused small NP building blocks strongly coupled. The growth procedure was shown as Scheme 1 in ESI. It should be mentioned that the final formed spherical Pd NPAs are very stable because they cannot be broken even if they are treated in a strong ultrasonic bath for about 1 h. This phenomenon implies that the small NP building blocks are strongly coupled, which may cause the formed Pd NPAs possess enhanced electrical properties and facilitate the electron transfer. The detailed formation process on such Pd NPAs is underway in our lab.

3.3. H_2O_2 detection using Pd NPAs modified electrode

Here we use the obtained spherical porous Pd NPAs as a catalyst to promote the reduction of H_2O_2 and measure the reduction current at a negative potential. Fig. 3 exhibits the amperometric response of Pd NPAs modified GCE with successive additions of H_2O_2 to 0.1 M pH 7.0 PBS at an applied potential of −0.45 V. Upon addition of an aliquot of H_2O_2 to the buffer solution, the reduction current increases steeply to reach a stable value. The

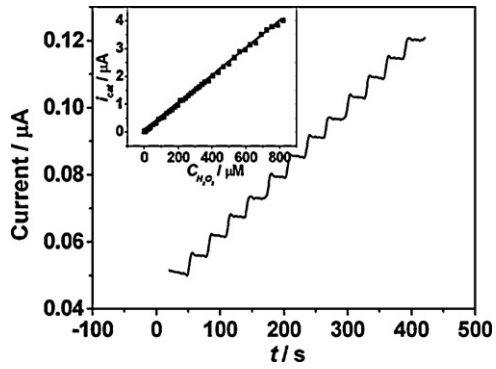

Fig. 3. Amperometric response of Pd NPAs modified electrode upon successive additions of 5 μL 1.0 mM H_2O_2 to 5.0 mL 0.1 M pH 7.0 N_2 saturated PBS at −0.45 V. Insets: calibration curve of H_2O_2 sensor with five reduplicate measurements.

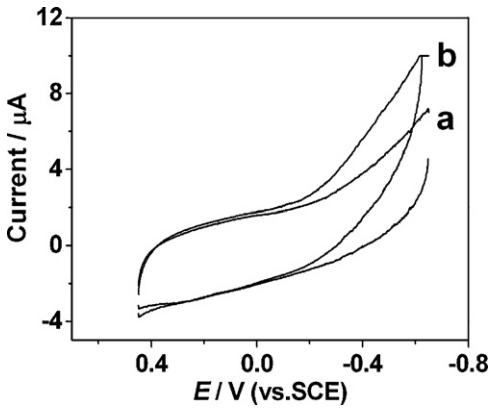

Fig. 4. CVs of GOx/Pd NPAs modified electrode in 0.1 M pH 7.0 PBS with oxygen saturated without (a) and with (b) 20 mM H_2O_2 at 100 mV/s, respectively.

electrode achieves 95% of the steady-state-current in less than 10 s, implying that the electrocatalytic response is very fast. The linear response range of the sensor to H_2O_2 concentration is from 1.0×10^{-6} to 8.2×10^{-4} M with a correlation coefficient of 0.9994 ($n = 40$) which is wider than 5.0×10^{-6} to 1.35×10^{-4} M based on C@Au composite (Zhu et al., 2011). The detection limit is estimated to be 6.8×10^{-7} M at a signal-to-noise ratio of 3 which is lower than 4.7×10^{-6} M of Ag nanoparticle-decorated poly(m-phenylenediamine) microparticles (Tian et al., 2011). The good detection performance is attributed to the enhanced activity of Pd NPAs. The reactivity of Pd NPs can often be correlated with the energy of the center of the *d* band and with their density of states (Hammer et al., 2000). In our Pd NPAs sample, the strong coupling among adjacent small NP building blocks will result in the sharp increase of electron density of states on the surface of NPAs, so the enhanced activity and good detection performance are observed.

3.4. Glucose detection using GOx and Pd NPAs

It was noted that upon addition of glucose to 0.1 M pH 7.0 air-saturated PBS, the shape of CV also changed with an increase of reduction current at GOx/Pd NPAs modified GCE. With the increasing concentration of glucose, the electrocatalytic response obviously increased. The previous reports focused on the glucose biosensor constructed by measuring the decrease of the cathodic current during the reduction of dissolved oxygen due to its consumption in the enzymatic reaction (Guilbault and Lubrano, 1973; Clark et al., 1962; Updike and Hicks, 1967). In our protocol, the response increased upon the addition of glucose. To clarify the mechanism of this protocol, the following experiment has been carried out. Curves a and b in Fig. 4 show CV signals of GOx/Pd NPAs modified electrode in 0.1 M pH 7.0 oxygen saturated PBS without and with 20 mM H_2O_2, respectively. It showed that the addition of H_2O_2 caused the increase of reduction signal. Thus the increased response formed not only from the electrochemical reduction of oxygen but also from the obtained H_2O_2 at the electrode surface. Because the oxygen was saturated in PBS solution, the oxygen concentration was fixed. With the increase of glucose, the forming H_2O_2 increased, leading the reduction response to increase.

According to the above mentioned experimental results, the mechanism in our designed protocol can be inferred and shown as Eqs. (1)–(4):

$$\text{Glucose} + \text{GOx(FAD)} \rightarrow \text{gluconolactone} + \text{GOx(FADH}_2\text{)} \quad (1)$$

$$\text{GOx(FADH}_2\text{)} + \text{O}_2 \rightarrow \text{GOx(FAD)} + \text{H}_2\text{O}_2 \quad (2)$$

$$\text{Pd} + \text{H}_2\text{O}_2 + 2\text{H}^+ \rightarrow \text{Pd}^{2+} + 2\text{H}_2\text{O} \quad (3)$$

$$\text{Pd}^{2+} + 2\text{e} \rightarrow \text{Pd} \quad (4)$$

3.5. Effecting factors

To improve the performance of the sensor, various factors influencing the response of the sensor were investigated, including the pH values of the buffer (Fig. S4A in ESI), the applied potential (Fig. S4B in ESI) and the volume ratio of GOx to Pd NPAs covered on the surface of the working electrode (Fig. S4C in ESI).

3.6. Amperometric response of glucose sensor

The amperometric response of glucose increased with increasing glucose concentrations at GOx/Pd NPAs modified GCE. Fig. 5 illustrated a typical current–time plot for successive additions of 5.0 μL of 0.04 M glucose to 5.0 mL of 0.1 M pH 7.0 PBS at an applied potential of −0.45 V. When an aliquot of glucose was added into the buffer solution, the reduction current rose steeply to reach a stable value, and achieved 95% of steady-state current in less than 10 s, indicating the fast diffusion of substrate from the bulk solution to the interface between GOx and Pd NPAs. When the concentration of glucose was over 22 mM, the amperometric response trended to a constant value.

Under the optimized experimental conditions the sensor showed a linearly increased amperometric response to glucose ranging from 4.0×10^{-5} to 2.2×10^{-2} M with a relative coefficient of 0.9991 ($n = 21$). The average relative standard deviation (RSD) of the plots was 4.6%. This linear range was much wider than the ranges of 0.25–19 mM for GOx in a single ZnO nanofiber (Ahmad et al., 2010), 1–20 mM for construction of mediatorless bi-enzymatic glucose biosensor based on organic inorganic hybrid (Manesh et al.,

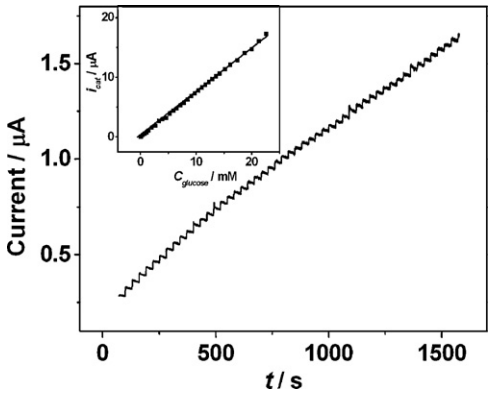

Fig. 5. Amperometric response of GOx/Pd NPAs modified GCE upon successive additions of 5 μL 0.04 M glucose to 5.0 mL 0.1 M pH 7.0 PBS at −0.45 V. Insets: linear calibration curve of glucose sensor with five reduplicate measurements.

2010) and 0.1–58 mM for nonenzymatic glucose sensor on nanostructure (Bai et al., 2010). It is well known that the diabetic glucose concentration is above 7.0 mM, which illustrated that the designed sensor was suitable for sensing of glucose in practical samples of diabetic patients. The detection limit of 6.1×10^{-6} M at a signal-to-noise ratio of 3 was also much lower than 180 μM based on GOx adsorbed on MCM-41 modified GCE (Dai et al., 2007) and 0.01 mM based on GOx immobilized on nitrogen-doped carbon nanotubes (Deng et al., 2009). The lower detection limit and wider linear range might be attributed to the following three reasons. One is the novel analytical method which used spherical porous Pd NPAs as an electron transfer transducer and the substitute of HRP. The second is that starch-stabilized Pd NPAs have an interaction with GOx due to the bonding effect and they have a good affinity with analytical substrate, favoring for the diffusion and enrichment of substrate. At glucose concentration higher than 2.2×10^{-2} M, the calibration curve shows a platform. The K_M^{app} value is also estimated to be 0.09 mM which is lower than 0.141 mM from iron oxide nanoparticles-chitosan composite (Kaushika et al., 2008) indicating the good affinity. The third is that the strong electron coupling among adjacent NP building blocks will enhance the electrical properties of Pd NPAs, facilitating the electron transfer process and the amplification of the detection signal.

3.7. Interferences

The amperometric responses for relevant physiological levels of glucose, ascorbic acid, acetaminophen, and uric acid at the GOx/Pd NPAs modified electrode at −0.45 V were compared. The amperometric responses were obtained by adding 0.5 mM interfering species in the solution containing 1.0 mM glucose. It was found that 0.5 mM uric acid and 0.5 mM p-acetaminophenol showed almost no interference with the determination of glucose and 0.5 mM ascorbic acid produced a relative response of about 7.5%, indicating these species coexisting in the sample matrix did not affect the determination of glucose and the sensor had good specificity.

3.8. Stability and reproducibility

The storage stability of the glucose biosensor in 0.1 M pH 7.0 PBS or air at 4 °C was examined by checking periodically their relative responses (the ratios of the catalytic currents detected at different times to the initial current value) in 0.1 M pH 7.0 PBS containing 1.0 mM glucose. The sensors could retain 90% of their initial activity to glucose within a storage period of 60 days in 0.1 M pH 7.0 PBS at 4 °C, while only 60% of activity to glucose was retained when stored in air at 4 °C.

The fabrication reproducibility of six electrodes, made independently, showed an acceptable reproducibility with a relative standard deviation (RSD) of 5.1% for the currents determined at a glucose concentration of 1.0 mM. With one sensor, the mean steady state current was 0.8 μA with a RSD of 3.2% for six determinations at a glucose concentration of 1.0 mM.

3.9. Practical sample determination

To evaluate its applicability, the electrode was used for the detection of the concentration of glucose in blood sample. The recovery measurements were first carried out. The recoveries for the assay of 1.0–10.0 mM glucose were between 95.7 and 105.1% for five detections, indicating the developed electrode had high accuracy in measuring the blood glucose.

The precision was performed by taking three samples: 40 μM (low concentration), 0.5 mM (middle concentration) and 20 mM (high concentration) glucose and each sample was measured for three times. The RSD of each sample was 6.3, 4.3 and 3.8, respectively indicating good precision.

Table 1
Determination of glucose concentrations in the blood sample.

Sample no.	Measured by the biosensor		Measured by HPLC	
	Concentrations (mM)	RSD (%)	Concentrations (mM)	RSD (%)
1	1.22	2.80	1.36	2.82
2	3.14	3.15	3.49	3.43
3	5.45	2.96	5.76	3.87
4	7.33	3.52	7.58	2.96
5	9.29	2.76	9.17	3.25

Each data is an average value of the response of five measurements for each sample.

Five blood samples were analyzed using five independently prepared electrodes. The obtained results were compared with those measured with high performance liquid chromatography (HPLC) (Table 1). It was shown that the values measured by the developed biosensor were in good agreement with the data from HPLC, showing a good accuracy, indicating that the glucose biosensor had a great potential for practical application for the analysis of glucose in real clinical samples.

4. Conclusions

In summary, spherical porous Pd NPAs have been successfully prepared by starch-assisted chemical reduction of H_2PdCl_4 at room temperature. Such Pd NPAs have good adhesion ability with electrode surface and do not need extra chitosan or Nafion to fix them. By directly dropping the suspension of those Pd NPAs on GCE, the H_2O_2 biosensor can be easily constructed. Furthermore, the sensitive and selective glucose biosensor is developed *via* co-depositing of such Pd NPAs and GOx on GCE. The proposed biosensor shows wider range and low detection limit and excellent performance for serum glucose level. This work demonstrates that the obtained spherical porous Pd NPAs can be served as an ideal substitute of HRP and provides a promising strategy to construct fast, sensitive, stable and anti-interferential amperometric biosensors for the detection of glucose, which is beneficial to the early diagnosis and control of diabetes. Further work on exploring proper nanostructured material for substitution of GOx is in progress.

Acknowledgements

This work was supported by the National Natural Science Foundation of China for the project (nos. 20875046, 21175069, 20871070 and 20901041), the Program for New Century Excellent Talents in University (NCET-09-0159). We greatly appreciate the financial support from the Priority Academic Program Development of Jiangsu Higher Education Institutions.

Appendix A. Supplementary data

Supplementary data associated with this article can be found, in the online version, at doi:10.1016/j.bios.2011.10.008.

References

Ahmad, M., Pan, C.F., Luo, Z.X., Zhu, J., 2010. J. Phys. Chem. C 114, 9308–9313.
Alayoglu, S., Nilekar, A.U., Mavrikakis, M., Eichhorn, B., 2008. Nat. Mater. 7, 333–338.
Astruc, D., Lu, F., Aranzaes, J.R., 2005. Angew. Chem. Int. Ed. 44, 7852–7872.
Bai, H.Y., Han, M., Du, Y.Z., Bao, J.C., Dai, Z.H., 2010. Chem. Commun. 46, 1739–1741.
Barman, T.E., 1985. Enzyme Handbook, vol. I. Springer-Verlay, New York, p. 234.
Berglund, G.I., Carlsson, G.H., Smith, A.T., Szoke, H., Henriksen, A., Hajdu, J., 2002. Nature 417, 463–468.
Breslow, R., 1995. Acc. Chem. Res. 28, 146–153.
Chattopadhyay, K., Mazumdar, S., 2000. Biochemistry 39, 263–270.

Clark, L.C., Lyons, C., 1962. Ann. N.Y. Acad. Sci. 102, 29–45.
Corma, A., González-Arellano, C., Iglesias, M., Sánchez, F., 2007. Angew. Chem. Int. Ed. 46, 7820–7822.
Cosnier, S., Lambert, F., Stoytcheva, M., 2000. Electroanalysis 12, 356–360.
Cosnier, S., Mousty, C., Cui, X.Q., Yang, X.R., Dong, S.J., 2006. Anal. Chem. 78, 4985–4989.
Crouch, E., Cowell, D.C., Hoskins, S., Pittson, R.W., Hart, J.P., 2005. Anal. Biochem. 347, 17–23.
D'Orazio, P., 2003. Clin. Chim. Acta 334, 41–69.
Dai, Z.H., Ni, J., Huang, X.H., Lu, G.F., Bao, J.C., 2007. Bioelectrochemistry 70, 250–256.
Delvaux, M., Walcarius, A., Demoustier-Champagne, S., 2005. Biosens. Bioelectron. 20, 1587–1594.
Deng, S.Y., Jian, G.Q., Lei, J.P., Hu, Z., Ju, H.X., 2009. Biosens. Bioelectron. 25, 373–377.
Enache, D.I., Edwards, J.K., Landon, P., Solsona-Espriu, B., Carley, A.F., Herzing, A.A., Watanabe, M., Kiely, C.J., 2006. Science 311, 362–365.
Ferri, T., Poscia, A., Santucci, R., 1998. Bioelectrochem. Bioenerg. 45, 221–226.
Fillon, Y., Verma, A., Ghosh, P., Ernenwein, D., Rotello, V.M., Chmielewski, J., 2007. J. Am. Chem. Soc. 129, 6676–6677.
Forrow, N.J., Bayliff, S.W., 2005. Biosens. Bioelectron. 21, 581–587.
Guilbault, G.G., Lubrano, G.L., 1973. Anal. Chim. Acta 64, 439–455.
Hammer, B., Nørskov, J.K., Bruce, C.G., 2000. Advances in Catalysis, vol. 45. Academic Press, San Diego CA, p. 71.
Haruta, M., 2005. Nature 437, 1098–1099.
Hashmi, A.S.K., Hutchings, G.J., 2006. Angew. Chem. Int. Ed. 45, 7896–7936.
Huang, J.S., Wang, D.W., Hou, H.Q., You, T.Y., 2008. Adv. Funct. Mater. 18, 441–448.
Huang, X., Tang, S., Zhang, H., Zhou, Z., Zheng, N., 2009. J. Am. Chem. Soc. 131, 13916–13917.
Kaushika, A., Khan, R., Solanki, P.R., Pandey, P., Alam, J., Ahmad, S., Malhotra, B.D., 2008. Biosens. Bioelectron. 24, 676–683.
Ksar, E., Surendran, G., Ramos, L., Keita, B., Nadjo, L., Prouzet, E., Beaunier, P., Hagège, A., Audonnet, F., Remita, H., 2009. Chem. Mater. 21, 1612–1617.
Lee, H., Habas, S.E., Somorjai, G.A., Yang, P., 2008. J. Am. Chem. Soc. 130, 5406–5407.
Li, Y.F., Bai, H.Y., Liu, Q., Bao, J.C., Han, M., Dai, Z.H., 2010. Biosens. Bioelectron. 25, 2356–2360.
Lim, S.H., Wei, J., Lin, J.Y., Li, Q.T., Kua, Y.J., 2005. Biosens. Bioelectron. 20, 2341–2346.
Lim, B., Jiang, M., Camargo, P.H.C., Cho, E.C., Tao, J., Lu, X., Xia, Y., 2009. Science 324, 1302–1305.
Malhotra, B.D., Chaubey, A., 2003. Sens. Actuators B 91, 117–127.
Manesh, K.M., Santhosh, P., Uthayakumar, S., Gopalan, A.I., Lee, K.P., 2010. Biosens. Bioelectron. 25, 1579–1586.
Mazumder, V., Sun, S., 2009. J. Am. Chem. Soc. 131, 4588–4589.
Min, B.K., Friend, C.M., 2007. Chem. Rev 107, 2709–2724.
Niculescu, M., Nistor, C., Frebort, I., Pec, P., Mattiasson, B., Csoregi, E., 2000. Anal. Chem. 72, 1591–1597.
Pandey, P.C., Upadhyay, S., Upadhyay, A.K., 2004. Sens. Actuators B 102, 126–131.
Shi, L.X., Lu, Y.X., Sun, J., Zhang, J., Sun, C.Q., Liu, J.Q., Shen, J.C., 2003. Biomacromolecules 4, 1161–1167.
Shoji, E., Freund, M.S., 2001. J. Am. Chem. Soc. 123, 3383–3384.
Si, R., Flytzani-Stephanopoulos, M., 2008. Angew. Chem. Int. Ed. 47, 2884–2887.
Tian, N., Zhou, Z.Y., Sun, S.G., Ding, Y., Wang, Z.L., 2007. Science 316, 732–735.
Tian, J.Q., Li, H.L., Lu, W.B., Luo, Y.L., Wang, L., Sun, X.P., 2011. Analyst 136, 1806–1809.
Updike, S.J., Hicks, G.P., 1967. Nature 214, 986–988.
Wang, J., 2008. Chem. Rev. 108, 814–825.
Wang, W., Li, Z.Y., Zheng, W., Yang, J., Zhang, H.N., Wang, C., 2009. Electrochem. Commun. 11, 1811–1814.
Yan, W.J., Wang, R., Xu, Z.Q., Xu, J.K., Lin, L., Shen, Z.Q., Zhou, Y.F., 2006. J. Mol. Catal. A-Chem. 255, 81–85.
Yang, L.L., Yang, Z.H., Cao, W.X., Chen, L., Xu, J., Zhang, H.Z., 2005. J. Phys. Chem. B 109, 11501–11504.
Yin, L., Liebscher, J., 2007. Chem. Rev. 107, 133–173.
Yu, J.H., Liu, S.Q., Ju, H.X., 2003. Biosens. Bioelectron. 19, 401–409.
Zecchina, A., Groppo, E., Bordiga, S., 2007. Chem. Eur. J. 13, 2440–2460.
Zhang, G., Shen, X., Yang.F Y., 2011. J. Phys. Chem. C 115, 7145–7152.
Zhou, P., Dai, Z., Fang, M., Huang, X., Bao, J., 2007. J. Phys. Chem. C 111, 12609–12616.
Zhu, W.L., Wang, Y.Y., Xuan, J., Zhang, J.R., 2011. J. Nanosci. Nanotechnol. 11, 138–142.